Ethanol formation from CO2 hydrogenation at atmospheric pressure using Cu catalysts: water as a key component

da Silva, A.H.M.; Vieira, L.H.; Santanta, C.S.; Koper, M.T.M.; Assaf, E.M.; Assaf, J.M.; Gomes, J.F.

Applied Catalysis B: Environmental 324 (2023) 122221

Contents lists available at ScienceDirect

Applied Catalysis B: Environmental

journal homepage: www.elsevier.com/locate/apcatb

Ethanol formation from CO_2 hydrogenation at atmospheric pressure using Cu catalysts: Water as a key component

Alisson H.M. da Silva [a,c], Luiz H. Vieira [a], Cássia S. Santanta [a,c], Marc T.M. Koper [c], Elisabete M. Assaf [b], José M. Assaf [a,*], Janaina F. Gomes [a,*]

[a] Chemical Engineering Department, São Carlos Federal University, São Carlos, São Paulo, Brazil
[b] São Carlos Institute of Chemistry, University of São Paulo, São Carlos, São Paulo, Brazil
[c] Chemistry Institute, Leiden University, Leiden, Netherlands

ARTICLE INFO

Keywords:
CO_2 hydrogenation
Ethanol
Water steam
Cu

ABSTRACT

The catalytic conversion of CO_2 can reduce its impact in the atmosphere and produce chemicals of industrial interest. Based on this, herein, ethanol formation from CO_2 hydrogenation with water was studied. Inspired by CO_2 electroreduction results, we show that ethanol can be formed at atmospheric pressure, using metallic Cu catalysts in the CO_2 hydrogenation with water steam ($CO_2 + H_2 + H_2O$) with selectivity of 84% and productivity of ~2 μmol.gcat^{-1}.h^{-1} at 190 °C. When only H_2O is used (without H_2), the same trend was observed. To the best of our knowledge, ethanol is reported for the first time to be synthesized at atmospheric pressure, using only CO_2 and water as reactants in a thermocatalytic process. ^{1}H NMR results showed that water (and deuterated water) hydrogenate CO_2 to form ethanol. CO-DRIFTS analyses revealed that water enhances the carbon-metal strengthening and this can explain why ethanol production is favored during the CO_2 hydrogenation.

1. Introduction

The atmospheric CO_2 concentration has increased by over 100 ppm in the last century, whereby more than 20 ppm has increased over the last ten years. This increase is mainly caused by the agriculture and industrial expansions that are essential for human needs, and therefore these activities cannot be quickly interrupted. The best strategy to reduce the impact of human activities is to convert CO_2 into desired products that can be reused by society. To this end, catalytic hydrogenation of CO_2 is one of the most promising applications due to its possibility of massively converting CO_2 into fuels and building blocks for the chemical industry. For example, the synthesis of chemicals with two or more carbons (C_{2+} compounds), as ethanol, is a desired reaction because it can both reduce the impact of this gas in the atmosphere and produce a chemical of high interest due to its broad applicability in the industry and our daily life.

Effective Cu-based catalysts have been used for CO_2 hydrogenation, such as modified industrial $Cu/ZnO/Al_2O_3$ [1,2], Cu/ZnO/M (M= Zr [3–5], Ce [6,7], Ti [8–10], Ga [11–13], Nb [14], and others [15,16]), and Pd-Cu [17,18], but mainly C_1 compounds (CO, CH_4, and methanol) are reported as products. Such an approach has already been applied for methanol synthesis on a large scale. George Olah Renewable Methanol plant in Reykjavik, Iceland, was the first company to produce ten ton$_{methanol}$/day from CO_2 and H_2 using heterogeneous catalysis and geothermal energy [19]. In contrast, the synthesis of higher alcohols, e.g., ethanol, from CO_2 hydrogenation is still far from a mature technology for industrial application because, differently from methanol synthesis, C-C coupling is needed to produce these compounds. The C-C coupling hampers the reaction pathway significantly, requiring catalysts that allow CO_2 and CO to be adsorbed strongly enough to prevent them from being desorbed as a product before being reacted, and not so strongly that the catalyst is not poisoned by the adsorption of carbon. Recently, many efforts have been dedicated to obtaining better catalytic performance in ethanol synthesis from CO_2 hydrogenation [20–26]. Applying noble metals like Pd and Iridium, high selective hydrogenation of CO_2 to ethanol is achieved (> 90%), although CO_2 conversion is relatively low (< 10 %) [21,23,27]. Cu-, Co-, and Fe-based catalysts, otherwise, shows higher CO_2 conversion (> 30%) but the ethanol selectivity is compromised (< 40 %) [28–30]. Unique performance was found on Cu@Na-Beta, where ethanol was 100% selective at 300 °C and 1.3 MPa with 8% CO_2 conversion [25].

Although a lot of advances have been achieved on the ethanol

* Corresponding authors.
E-mail addresses: mansur@ufscar.br (J.M. Assaf), janainafg@ufscar.br (J.F. Gomes).

https://doi.org/10.1016/j.apcatb.2022.122221
Received 2 September 2022; Received in revised form 12 November 2022; Accepted 25 November 2022
Available online 26 November 2022

synthesis from CO_2 hydrogenation, low productivity, low conversion, severe reaction conditions, and/or high costs involved in the process inhibit practical applications. One of these problems is using H_2 as a hydrogen source for CO_2 hydrogenation. CH_4 steam reforming is the primary source to produce H_2, and the costs already involved in the production of H_2 make the conventional CO_2 hydrogenation to ethanol ($2CO_2 + 6\ H_2 \leftrightarrow C_2H_5OH + 3\ H_2O$) economically unfeasible. Furthermore, the CH_4 is mainly obtained from fossil fuels, which impairs the sustainability of the process. A promising strategy is using H_2O to partially (or fully) suppress the use of H_2 as a hydrogen source [31]. CO_2 electroreduction already uses this approach, and it is well known that ethanol and other C_{2+} compounds can be synthesized from CO_2 and H_2O, applying metallic Cu as the catalyst [32,33]. However, the high costs due to the overpotentials required for producing these chemicals also inhibit industrial applications.

In CO_2 hydrogenation, water is commonly avoided because it can sinter and oxidize the active phase [34,35], and only a few works study the impact of water on feed gas. He et al. [36] showed that higher alcohols (C_2-C_4) were synthesized at 80 bar ($H_2/CO_2 = 3/1$) and 140 °C applying Pt/Co_3O_4 in a batch reactor containing water as the solvent. They showed that water was responsible for promoting the reaction kinetically. Zhao et al. [37] performed CO_2 hydrogenation with water steam over a commercial $Cu/ZnO/Al_2O_3$ catalyst with the assistance of negative corona discharge plasma and showed that only ethanol was detected as the liquid product at 1 bar and 160 °C. Curiously, in the CO_2 hydrogenation with H_2 applying the industrial $Cu/ZnO/Al_2O_3$ catalyst, merely methanol and CO are produced (only C_1 compounds) [38–40]. Koishybay and Shantz [41] have shown that the water provides the hydroxyl group in the synthesis of methanol from partial oxidation of methane, which suggests that water plays an essential role in synthesizing alcohols. In the same direction, Wang et al. [42] reported strong evidence of methanol synthesis enhancement from CO_2 hydrogenation over Cu-ZnO-ZrO_2 (CZZ) catalysts by increasing the methanol selectivity and the methanol yield, adding a certain amount of water to the feed gas. So, as commonly seen in the CO_2 electroreduction approach, water in the reactional medium may play an essential role in synthesizing alcohols and C_2 compounds via thermocatalysis although its impact is poorly investigated in literature and more evidence of the water impact in the products distribution of the CO_2 hydrogenation are still necessary.

Here, we investigated the impact of water on ethanol production from CO_2 hydrogenation with water steam at atmospheric pressure, temperatures between 170 and 240 °C, and applying metallic Cu catalysts. Our results showed that the water steam can favor the formation of ethanol from CO_2 while in its absence only CO and methanol were observed (C_1 compounds) on Cu catalysts. Thermodynamics were also discussed here. CO-DRIFTS indicate that water steam enhances the carbon-metal strengthening and this can explain why ethanol production is favored in the CO_2 hydrogenation with water.

2. Experimental

2.1. Catalyst synthesis

2.1.1. Preparation of Cu_{prec}

CuO powder was synthesized via the precipitation method. In a typical procedure, 3.80 g of $Cu(NO_3)_2 0.3\ H_2O$ (99 %, Sigma-Aldrich) were dissolved in 20 mL of deionized water. Then this solution containing Cu ions was slowly dripped into 400 mL of 0.1 M $NaHCO_3$ under constant stirring and at a temperature of 70 °C. The pH of the solution was controlled to be between 7 and 8. Decreases in pH due to the addition of the Cu precursor were compensated by the dropwise of a 0.5 M $NaHCO_3$. After completing the Cu precursor addition, the solution was aged for 2 h. Finally, the solid was separated from the supernatant by filtration, followed by washing (with at least 2 L of deionized water), dried at 80 °C for 12 h, and calcined for 5 h at 350 °C using a heating rate of 2 °C/min. Before the catalyst was used in the CO_2 hydrogenation, the CuO powder was reduced in situ with H_2, resulting in the metallic Cu powder, called $Cu_{prec.}$.

2.1.2. Preparation of Cu_{calc}

CuO powder was synthesized by direct calcination of $Cu(NO_3)_2 0.3\ H_2O$. Typically, 3.80 g of $Cu(NO_3)_2 0.3\ H_2O$ (99 %, Sigma-Aldrich) were placed in a porcelain crucible, and the nitrate was calcined for 5 h at 350 °C using a heating rate of 2 °C/min. Before the catalyst was used in the CO_2 hydrogenation, the CuO powder was reduced in situ with H_2, resulting in the metallic Cu powder, named Cu_{calc}.

2.1.3. Preparation of Cu_{cubes}

Cu_xO was synthesized according to the procedure proposed by Chang et al. [43]. In a typical procedure, 1 mL of 1.2 M $CuSO_4$ ($CuSO_4$, 99 %, Synth) was quickly added to a round bottom flask with 0.2 M $C_6H_5Na_3O_7$ ($C_6H_5Na_3O_7 0.2\ H_2O$, 99%, Synth) at 25 °C and under vigorous stirring. After 5 min, 1 mL of 4.8 M NaOH (NaOH, 99 %, Aldrich) was added to the solution. The solution immediately turned turbid blue, indicating $Cu(OH)_2$ precipitation. After another 5 min, 1 mL of 1.2 M ascorbic acid was added to the solution as a reducing agent. The color of the solution rapidly turned from turbid blue to yellowish-brown, indicating the formation of Cu_2O. The solution was kept in a water bath and under vigorous stirring for another 30 min. The solid formed was filtered and washed with deionized water. Finally, the filtered solid was dried for 2 h at 80 °C. Before the catalyst was used in the CO_2 hydrogenation, the Cu_xO powder was reduced in situ with H_2, resulting in the metallic Cu powder, named Cu_{cubes}.

2.2. Catalyst characterization

Scanning electron microscopy (SEM) images were obtained in an Apreo SEM (ThermoFisher Scientific) with an acceleration voltage of 15 kV and an electron beam current of 0.4 nA.

The specific surface areas were measured in a Micromeritics ASAP 2020 instrument according to the traditional B.E.T method using N_2 physisorption at − 196 °C. The samples were pre-treated under vacuum for 2 h at 200 °C. Before the specific surface area be measured, the Cu_xO was reduced for 1 h at 300 °C.

The temperature-programmed reduction (TPR) and temperature-programmed desorption (TPD) analysis were performed on a Micromeritics ChemiSorb 2750 equipped with a thermal conductivity detector (TCD). First, 150 mg of catalyst were inserted in a U-tube reactor and pre-treated for 60 min at 300 °C in a flow of H_2 (40 mL/min). For the TPR experiment, the surface of the metallic Cu catalyst was oxidized to Cu^+ by flowing 10 % N_2O/Ar (25 mL/min) for 30 min at 30 °C followed by surface purging with Ar for additional 30 min at the same temperature. Afterward, the catalyst's surface was reduced during heating from 30° to 450°C in a 10 % H_2/Ar mixture at a flow rate of 25 mL/min. For the H_2-TPD experiment, the pre-reduced catalyst surface was kept under H_2 flow at 30 °C for 30 min, followed by purging with Ar for 30 min to remove any physisorbed H_2. Afterward, the desorption was monitored by heating the reactor from 30° to 800 °C at an Ar flow rate of 25 mL/min.

2.3. Thermocatalytic CO_2 hydrogenation

2.3.1. CO_2 hydrogenation with H_2

The catalytic tests for CO_2 hydrogenation with H_2 were conducted in a bed stainless-steel flow reactor. Before the reaction, the catalyst precursor was reduced under H_2 flow (30 mL/min) at 300 °C for 1 h. Then, the reactor was fed with a gas mixture of H_2 and CO_2 with a volume ratio of $H_2/CO_2 = 1/1$ (50 mL/min). The reaction products and no converted reactants were evaluated online with a gas chromatograph Agilent Technologies-7890A, equipped with two detectors (one TCD and one FID), one molecular sieve (HP-MOLESIEVE), and 2 columns (one HP-PONA, and one HP-Plot/Q).

2.3.2. CO_2 hydrogenation with water steam

The catalytic tests for CO_2 hydrogenation with water steam were carried out in a tubular fixed bed reactor (Ø 5 mm). A scheme of the reaction apparatus is shown in Fig. S1. Before the reaction was carried out, the catalyst precursor was reduced under H_2 flow (30 mL/min) at 300 °C for 1 h. In a typical test, CO_2 was bubbled into a saturator containing deionized water at 80 °C. CO_2 and saturated water were dragged to the reactor, where the catalyst was located. All piping lines were heated with electrical heating tapes (up to 110 °C) to prevent water vapor condensation. For the tests with the mixture of $CO_2 + H_2 + H_2O$, H_2 flow was added to the reactor flow. The flow composition was $CO_2/H_2/H_2O = 1/1/1$ (total flow of 75 mL/min) or $CO_2/H_2O = 1/1$ (total flow of 50 mL/min). The temperature of the saturator was determined using Raoult's law and Antoine equation. With Raoult's law, vapor pressure of a desired composition can be find: $y = P_{vap}/P_{total}$, where y is the water steam composition in the gas flow. With Pvap, the temperature of the saturator can be determined via Antoine equation: $Pvap = A - B/(C-T)$, where T is temperature, A = 5.08354, B = 1663.125, and C = −45,622 are constants obtained from Bridgeman and Aldrich [44]. The flow of products and unconverted water and CO_2 were dragged to the reactor outlet, where the liquid phase was condensed and retained, while the gaseous phase was taken for in-line analysis using chromatography in the gas phase (GC). Ethanol was detected in the condensed liquid phase. The apparatus used to analyze the gaseous and liquid products was a GC Shimadzu 2014, equipped with three detectors (two TCDs and one FID) and 6 columns (two Porapak-Q, one Porapak-N, one MS-13X, one MS-5A, and one Stabilwax). Products selectivity was calculated as following:

$$Selectivity_i(\%) = product_i \Big/ \sum product;$$

$$Productivity_i(\mu mol \cdot g^{-1} \cdot h^{-1}) = mols_i \Big/ g_{cat.} \cdot t,$$

where i is the specific product, $g_{cat.}$ is the grams of catalyst used, and t is the reaction time.

The ^{1}H-NRM analysis was carried out in a Ascend™ 600 Bruker spectrometer using 600 MHz of frequency. Typically, 540 μL of the sample were mixed with 60 μL of D_2O solution containing 5 mM dimethyl sulfoxide (DMSO) as an internal standard. The spectra were collected with sixteen seconds of relaxation time between the pulses to allow for complete proton relaxation. Water suppression mode was used. MestreNova software was used for data processing.

2.4. Electrochemical methods

2.4.1. Electrodes preparation

The Cu disk electrode (99.99 %, trace metals basis, Mateck) with 1 cm of diameter was polished with alumina suspension followed by electropolishing at + 3 V vs. Cu for 10 s in 66 % of H_3PO_4. Ultrapure water was used to rinse the electrode after each procedure. Cu nanocubes were synthesized as described by Roberts, Kulh, and Nilsson [44]. Briefly, the Cu disk, as prepared before, was cycled 4 times at 5 mV/s from − 1.2 V to + 0.9 V vs. RHE in an electrolyte of 0.1 M $KHCO_3$ containing 4 mM KCl. The electrolyte was saturated with CO_2 for at least 15 min before the procedure started.

2.4.2. CO_2 electrochemical reduction test

CO_2 electrochemical reduction was performed as described in our previous paper [45]. Typically, CO_2 was continuously fed at a flow rate of 10 mL/min in a homemade H-cell (made of polyether ether ketone – PEEK) containing 0.1 M $KHCO_3$ as an electrolyte. An anionic exchange membrane (AHO, AGC Inc.) was used to separate the working-electrode compartment from that of the counter-electrode. Each compartment was filled with 10 mL of electrolyte. DSA was used as the counter electrode. All potentials measured against the Ag/AgCl/KCl_{sat}, used as reference electrode, were converted to RHE values according to the Nernst Equation ($E_{RHE} = E_{Ag/AgCl(KClsat.)} + 0.197 + 0.059$ pH). Biologic SP-300 was the potentiostat used to control the potential of the working-electrode. Liquid and gaseous products were analyzed by HPLC and GC, respectively.

2.4.3. Electrochemically active surface area (ECSA) measurements

ECSA was measured as described by Kanan and co-workers [46,47]. Briefly, the double-layer capacitance was obtained by performing cyclic voltammetry at scan rates of 100, 80, 60, 40, 20, and 10 mV/s in the double layer region (especially between −0.05 V and −0.35 V vs. RHE). 0.1 M $HClO_4$, Pt mash, and RHE were used as the electrolyte, counter electrode, and reference electrode, respectively. Considering that the number of electrochemically active sites is proportional to the double-layer capacitance value, the roughness factors (RF) of the electrodes were obtained by normalizing the measured capacitances for the flat polycrystalline Cu electrode (conventionally assumed as RF = 1).

3. Results and discussion

3.1. Catalytic performance of ethanol synthesis in the absence or presence of water

Fig. S2 shows the products distribution of the CO_2 hydrogenation ($CO_2/H_2 = 1$, v/v) on monometallic Cu catalyst at 1 bar (Fig. S2a) and 30 bar (Fig. S2b). The only products detected in the temperature range (160–260 °C) were CO and methanol. Increasing the pressure to 30 bar (Fig. S2b), both methanol and CO production were higher than those at 1 bar (Fig. S2b), but CO was similarly found as the main product. Ethanol and other C_{2+} products were not formed in detectable amounts at both pressures. These results agree with several works that show that C-C coupling is not favored on Cu active sites in CO_2 hydrogenation with H_2 [15,48,49].

Differently from CO_2 hydrogenation in gas-phase, ethanol and other C_{2+} compounds synthesis from CO_2 electroreduction are widely reported in the literature using an aqueous electrolyte saturated with CO_2 and applying monometallic Cu as electrode [32,33]. To compare with the results in the gas phase, Cu powder (the same catalyst used in Fig. S2) deposited on a carbon paper was used as the electrode for ethanol synthesis from CO_2 electroreduction at − 0.9, − 1.0, and − 1.1 V vs. reversible hydrogen electrode (RHE) in a CO_2-saturated $KHCO_3$ (0.1 M) electrolyte. In addition, conventional Cu_{disk} polycrystalline and Cu_{cubes}, synthesized by oxidation-reduction treatment (SEM image is presented in Fig. S3), were also applied to verify the impact of the catalytic surface area and the crystalline phase in the ethanol productivity. CO, ethanol, and ethylene were the main compounds detected for all electrodes. However, here we will present only the results of the liquid ethanol product, which is the focus of this work. Fig. 1 shows that ethanol was formed on all investigated catalysts and potentials applied. Cu_{cubes} was the electrode that presented the best catalytic performance for ethanol synthesis due to the preferential exposure of {100} facets in cubes [50]. Notably, {100} facets are essential features for C-C coupling from CO_2 in the presence of water [32,33,51–53], and thus it is reasonable that ethanol synthesis was more favored on Cu_{cubes} than on polycrystalline Cu_{disk} and Cu_{powder} catalysts. On the other hand, when comparing the results between Cu_{powder} and Cu_{disk}, the best performance in terms of ethanol productivity can be related to the active surface area (inferred here through the roughness factor, RF, shown in Fig. S4 and Table S1), among other factors out of the scope of the present work. The ratio between the RF of Cu_{powder} and that of Cu_{disk} was about 16. Thus, it was expected that a higher amount of ethanol could be synthesized applying Cu_{powder} than Cu_{disk}.

The differences observed in the results obtained in electrocatalysis and thermocatalysis are intriguing, suggesting that reaction conditions can lead to different product distributions (e.g., using an aqueous solution in the electrocatalytic system). Considering that ethanol can be synthesized on Cu materials in the CO_2 electrorreduction approach using

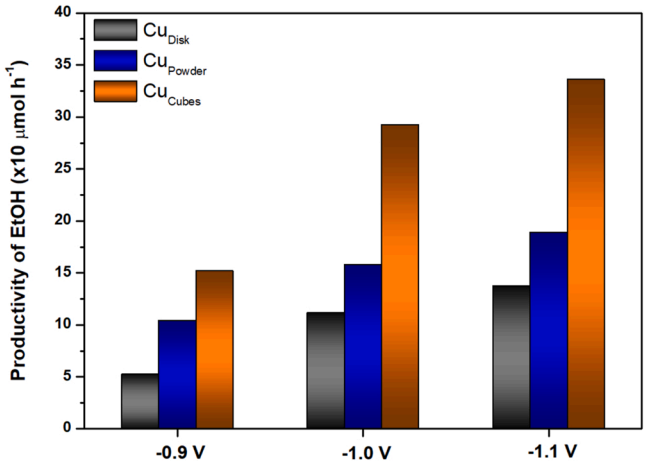

Fig. 1. Productivity of ethanol for Cu_{Disk} (black bars), Cu_{Powder} (blue bars), and Cu_{Cubes} (orange bars) at − 0.9 V, − 1.0 V, and − 1.1 V vs RHE. Reaction conditions: 10 mL of electrolyte (CO_2-saturated 0.1 M $KHCO_3$), 1 h of electrolysis.

an aqueous electrolyte (Fig. 1), CO_2 hydrogenation (in gas-phase) was performed as same as performed in Fig. S2a but adding water steam in the feed gas, and the results are shown in Fig. 2. Unlike Fig. S2a, Fig. 2 shows that ethanol could be detected when CO_2 hydrogenation with water steam was performed at 1 bar over metallic Cu catalyst. A typical chromatogram obtained from an injection of the condensed liquid (non-converted water containing liquid products) collected after the flow reactor is shown in Fig. S5a. It is interesting to note that the selectivity to ethanol could reach about 90 % at 170 °C and 180 °C, decreasing drastically at temperatures up to 220 °C. About the productivity, methanol and ethanol augmented when the temperature was increased from 170 °C to 200 °C and decreased at temperatures above 210 °C. It is important to mention that unlike CO_2 hydrogenation with H_2 at 30 bar where the CO_2 conversion can reach about 7% (Fig. S2b), CO_2 conversion is thermodynamically limited when the reaction is carried out at 1 bar. Therefore, about 0.1 % is converted for CO_2 hydrogenation with H_2 at 1 bar (Fig. S2a) and less than 0.1% is observed when water is added to the feed stream (Fig. 2). Further discussions about the thermodynamics will be presented in Section 3.3. Different GHSV values were also evaluated – 6000, 9000 or 12,000 $mL.g^{-1}.h^{-1}$ – and the product selectivity and productivity did not change, confirming that the tests were under the kinetic regime.

In parallel with the decline in productivity for alcohols, there was an increase in the productivity for CO. This species is considered one of the

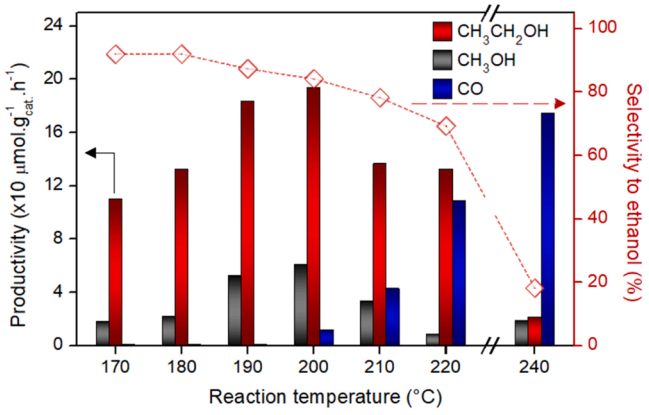

Fig. 2. Productivity of methanol (black bars), ethanol (red bars), CO (blue bars), and selectivity to ethanol between 170 °C and 240 °C. Reaction conditions: $m_{cat.}$ = 500 mg, $CO_2/H_2/H_2O_{(g)}$ = 1/1/1 (75 $mL.min^{-1}$), GHSV = 9000 $mL.g^{-1}.h^{-1}$, P = 1 bar.

key intermediaries in proposed reaction mechanisms for ethanol synthesis [32,33,54,55]. Therefore, the presence of adsorbed CO is essential for the synthesis of ethanol. However, the formation of CO as a reaction product means that CO produced in situ by the hydrogenation of CO_2 is desorbing rather than remaining adsorbed on the surface and being further hydrogenated for the formation of ethanol. In this work, 180–200 °C is the range of temperature that most favors the formation of ethanol. It is hard to compare the catalytic activity showed in this work with previous results in the literature as the reaction conditions applied here are not commonly used: 1 bar and adding water in the feed stream. However, a summary of reaction conditions, ethanol selectivity, CO_2 conversion, etc., of several recent works focused on ethanol formation from CO_2 hydrogenation are presented in Table S2.

The role of water as a hydrogen donor was clarified by carrying CO_2 hydrogenation with water steam in the absence of H_2 flow, and results are shown in Fig. S6. Interestingly, the same trend of methanol, ethanol, and CO productivity was observed. To the best of our knowledge, here we show for the first time that ethanol can be synthesized at atmospheric pressure, applying metallic Cu catalyst and using only CO_2 and water as reactants in a thermocatalytic process. A thermodynamic evaluation of the reaction and the catalyst deactivation will be discussed later in Section 3.3. Ethanol productivity in the absence of H_2 was slightly lower than that of the reaction with H_2, which indicates that the ethanol synthesis is mainly produced via $CO_2 + H_2O$. More insights about the water involvement in the synthesis of ethanol will be shown in Section 3.2.

Inspired by the electrocatalytic results (Fig. 1), CO_2 hydrogenation with water steam (without H_2 flow) was also performed in Cu catalysts with different surface areas and Cu_{cubes}. This study makes it possible to understand the influence of the surface area and the crystalline phase in ethanol synthesis in a thermocatalytic process as observed in electrocatalysis. Fig. 3 shows the ethanol productivity at 170 °C, 190 °C, and 210 °C by applying Cu catalysts obtained from (i) direct calcination of $Cu(NO_3)_2$, named $Cu_{calc.}$; (ii) precipitation of $Cu(OH)_2$ followed by calcination, named $Cu_{prec.}$; and (iii) controlled synthesis of Cu_2O to produce Cu nanocubes, as described by Chang et al. [43]. Before the reaction was carried out, Cu_xO was reduced in situ to Cu at 300 °C with H_2 for 1 h. Ethanol productivity decreased in the following order: $Cu_{cubes} > Cu_{prec.} > Cu_{calc}$. The differences can be partially justified by the material's surface areas. Cu_xO surface area was found to be 27 $m^2/g_{cat.}$ for Cu_{cubes}, 20 $m^2/g_{cat.}$ for $Cu_{prec.}$, and 11 $m^2/g_{cat.}$ for Cu_{calc}. Higher surface area may result in a higher amount of exposed Cu sites for CO_2 hydrogenation, which can lead to higher ethanol production. When the ethanol productivity was normalized by Cu_xO surface area (m^2_{Cu}) rather than of catalyst mass ($g_{cat.}$) (Fig. 3b), it became clear that $Cu_{prec.}$ and $Cu_{calc.}$ show similar results in terms of ethanol productivity. These data show that, for Cu_{prec} and Cu_{calc}, ethanol productivity depends directly on the Cu_xO surface area. On the other hand, ethanol productivity on Cu_{cubes} remains higher than on $Cu_{prec.}$ and $Cu_{calc.}$, even considering the surface area of the catalysts, which suggests that an additional feature in the Cu_{cubes} is acting to improve its catalytic performance. SEM images of Cu_{cubes} synthesized in this work are presented in Fig. S7. It is possible to see regular nanocubes with 47 ± 5 nm of edges, like those produced by Chang et al. [43], who also showed by HR-TEM that these nanocubes are {100} facets. Further surface characterization of the Cu nanocubes can be found in the work of Chang et al. [43]. Therefore, as evidenced in the CO_2 electroreduction approach, {100} facets preferably exposed in the Cu_{cubes} are also crucial in the hydrogenation of CO_2 with water steam. Similar to what was observed in Fig. 2 in electrocatalysis, ethanol synthesis from CO_2 and water steam is both area- and crystalline structure-sensitive.

3.2. Water involvement in the ethanol synthesis

Since the ethanol productivity is relatively low using only CO_2 and water in the thermocatalytic process, a natural question concerns the

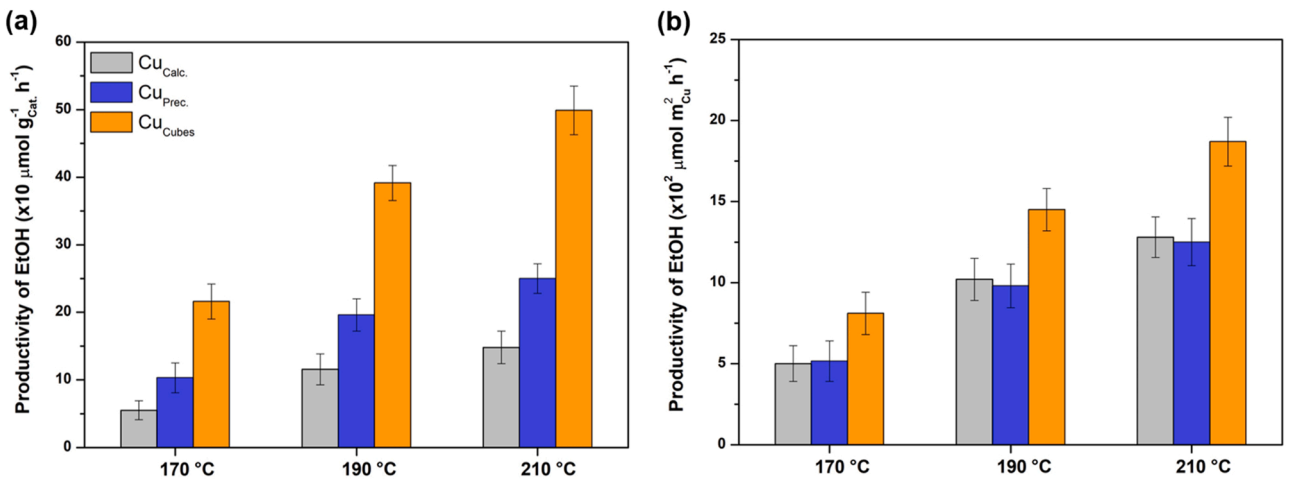

Fig. 3. Productivity of ethanol (a) per $g_{cat.}$ and (b) per m^2_{Cu} for $Cu_{Calc.}$ (gray bars), $Cu_{Prec.}$ (blue bars), and Cu_{Cubes} (orange bars) at 170 °C, 190 °C, and 210 °C. Reaction conditions: $m_{cat.}$ = 500 mg, $CO_2/H_2O_{(g)}$ = 1/1 (50 mL.min^{-1}), GHSV = 6000 mL.g^{-1}.h^{-1}, P = 1 bar.

possibility of the ethanol synthesis occurring by the reaction between the CO_2 and hydrogen chemisorbed on Cu, from the previous reduction step of Cu_xO to Cu with H_2. To investigate this possibility, H_2-TPD was performed on the Cu catalyst. In this analysis, no H_2 desorption was detected (Fig. S8a) after the reduction step, indicating that no residual hydrogen was chemically adsorbed on the Cu surface when the CO_2 hydrogenation reaction started. To confirm the reliability of these results, Cu^+ from pre-step oxidation of Cu with N_2O was studied by H_2-TPR. Fig. S8b shows hydrogen consumed in the Cu^+ to Cu^0 reduction process, attesting to the detection capability of the employed equipment at the investigated scale.

The involvement of water in the CO_2 hydrogenation was studied by ^{1}H NMR. CO_2 hydrogenation was performed with H_2O and, additionally, with a mixture of D_2O/H_2O steam at 190 °C, and the condensed liquid products were analyzed by ^{1}H NMR. It is essential to point out that before the reaction was carried out and to prevent misinterpretation of data, the natural exchange between hydrogen and deuterium in the ethanol molecule was investigated by preparing a standard ^{1}H NMR sample with 1 mmol/L in D_2O, which was aged for three days. The results show that triplet and quadruplet generated by CH_3 and CH_2 coupling, respectively, were not affected by D_2O, but the singlet generated by OH group (expected at ~2.61 ppm) presents an exchange to form OD in the presence of D_2O (Fig. S9 and Supplementary Note 1). So, natural exchange in CH_3 and CH_2 groups in solution between deuterium and the hydrogen from ethanol formed from CO_2 hydrogenation will not be considered here. Fig. 4 illustrates the multiplets and singlets generated by the couplings of the three non-equivalent hydrogen atoms present in ethanol and compares the spectra of condensed products of H_2O (black lines) and D_2O/H_2O containing reaction (blue lines). The characteristic triplet, generated by the coupling of hydrogen in CH_3 with the two hydrogens in CH_2, decreased its intensity when the reaction was carried out in the presence of D_2O. A doublet emerged, indicating the partial substitution of hydrogen by deuterium in the CH_2 group. The same effect was observed in the quadruplet generated by hydrogen in CH_2 with the three hydrogens in CH_3, indicating the partial substitution of hydrogen by deuterium in the CH_3 group. As mentioned before, the complete disappearance of the singlet, generated by the hydroxyl group of ethanol, can not be consistently attributed to substitution during reaction due to the natural exchange observed. The signal decreasing and the appearance of lower multiplicity peaks in $CO_2/H_2O/D_2O$ reaction in relation to CO_2/H_2O indicate the presence of partially deuterated molecules in two non-equivalent hydrogen positions of ethanol (CH_3 and CH_2), attesting that water is responsible for providing atomic hydrogen during the reaction. Additionally, as shown before, when the reaction was carried out

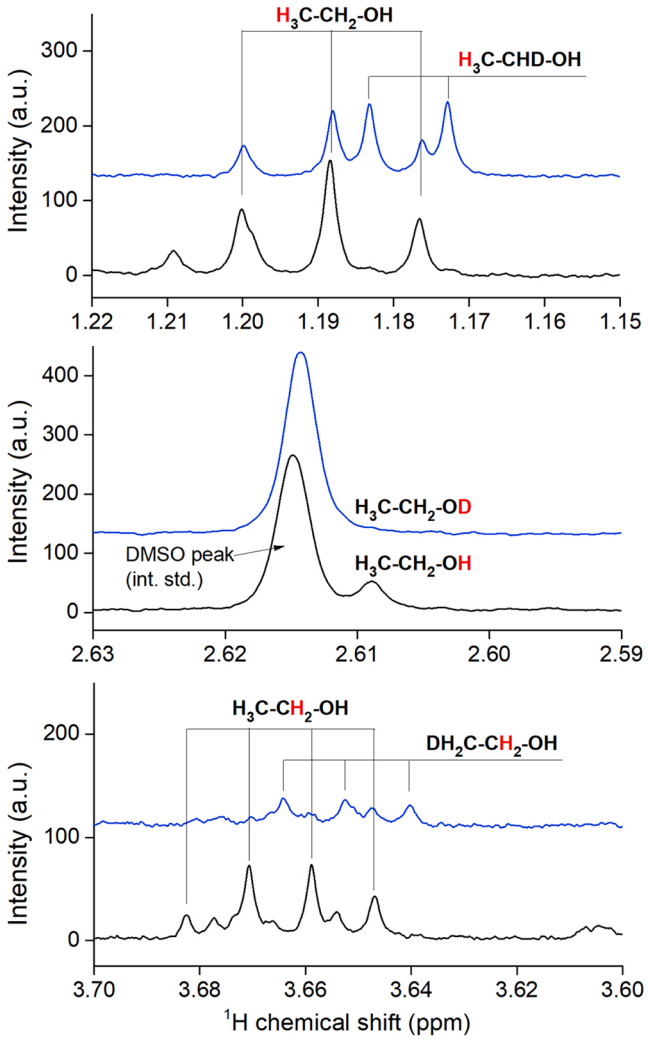

Fig. 4. ^{1}H NMR spectra of condensed products from CO_2 hydrogenation in the presence of H_2O (black lines) and H_2O/D_2O (blue lines). Reaction conditions: T = 190 °C, $m_{cat.}$ = 500 mg, $CO_2/H_2O_{(g)}$ = 1/1 (50 mL/min), P = 1 bar.

in a flow of $CO_2/H_2O/H_2$ (Fig. 2), no considerable increase in the production of ethanol was observed in relation to the use of CO_2/H_2O flow (Fig. S6), revealing that water is the primary hydrogen source to produce ethanol at the investigated conditions.

3.3. Thermodynamics discussion

The thermodynamic is one of the key questions about ethanol synthesis from CO_2 and water. Considering the global reaction: $2CO_{2(g)} + 3\ H_2O_{(g)} \rightarrow C_2H_5OH_{(g)} + 3\ O_{2(g)}$, it results in a reaction with high endothermic energy ($\Delta H = 1277.3$ kJ/mol). Under the reaction conditions applied in this work, ethanol might not be formed from the direct hydrogenation of CO_2 with water steam. In fact, some experimental insights indicate that ethanol can be formed from a different path. After the reduction step, it was possible to see by bare eyes that the catalyst was fully brownish, characteristic of metallic copper, while the catalyst was majority blackish after the reaction with water, indicating surface oxidation during the reaction. The material surface oxidation was also seen experimentally by the deactivation of the catalyst over time, as shown in Fig. 5a. Specifically, using a fresh catalyst sample, the ethanol productivity was practically suppressed after 3 h. However, when the same sample was reactivated, by reducing it again with H_2 at 300 °C for 1 h, ethanol synthesis was again detected (schematically exemplified in Fig. 5b). However, a lower productivity was observed than the fresh catalyst was used. This decay in productivity comparing both situations can be related to reducing the surface area. The surface area of the metallic Cu was measured to be 8.7 m^2/g, while the same material reactivated was 2.2 m^2/g, about 4 times smaller than the fresh sample. The same behavior was also observed for the second reactivation, although the decay in the ethanol productivity was smaller. This can again be explained by the surface area. The metallic surface area was measured to be 1.8 m^2/g, a value close to the measured before, so a strong decay is not expected as seen for the first reactivation. For the third reactivation, similar ethanol productivity was observed compared to the second reactivation, which was expected as the same metallic surface area was measured.

The deactivation observed in Fig. 5a indicates that Cu^0 is oxidized over time to Cu^{2+} and/or Cu^+ by water reduction, $Cu + H_2O \leftrightarrow CuO + H_2$, $2Cu + H_2O \leftrightarrow Cu_2O + H_2$. The oxidation of Cu by the presence of water leading to its deactivation has been studied by different groups. For example, Prašnikar and Likosar showed that the water formed in-situ from CO_2 hydrogenation to methanol increased the Cu deactivation rate [56,57]. In the same direction, Chen *et. al* showed by in-situ DRIFT and DFT calculation that the reduction of ethyl acetate on Cu is strongly affected by water adsorption [58]. More specifically, the active species of Cu^+ on the surface has preferred the adsorption of H_2O over the ethyl acetate molecule leading to a rapidly decreasing in the conversion ratio of ethyl acetate. At this moment, we do not have yet evidence whether Cu^0, copper oxides or a mixture of Cu^0/copper oxides is the active site for the ethanol formation in the catalytic reaction that we presented in this work. It is well known that Cu^+ is an important active site for methanol synthesis from CO_2 hydrogenation [59]. So, Cu^+ probably also plays an important role in the formation of ethanol. In this way, H_2O might also adsorb strongly on the catalyst surface, as observed by *Chen* et al. [58], favoring its deactivation.

With the oxidation of Cu metallic, hydrogen is formed in-situ by the water reduction which might drastically decrease the energy needed to form ethanol, turning the reaction exothermic. Specifically, the ethanol synthesis considering H_2 as the reducing agent ($2CO_{2(g)} + 6\ H_{2(g)} \rightarrow C_2H_5OH_{(g)} + 3\ H_2O_{(g)}$) has a $\Delta H = -173.5$ kJ/mol. So, combining the total oxidation reaction of Cu and the ethanol synthesis from CO_2 and H_2, we can write the global reaction for ethanol synthesis from CO_2 and water steam applying metallic copper as the catalyst, as shown in Eq. 3.

$$6Cu_{(s)} + 6\ H_2O_{(g)} \rightarrow 6CuO_{(s)} + 6\ H_{2(g)}\ \Delta H = 507\ \text{kJ/mol} \quad (1)$$

$$2CO_{2(g)} + 6\ H_{2(g)} \rightarrow C_2H_5OH_{(g)} + 3\ H_2O_{(g)}\ \Delta H = -173{\cdot}5\ \text{kJ/mol} \quad (2)$$

$$6Cu_{(s)} + 2CO_{2(g)} + 3\ H_2O_{(g)} \rightarrow C_2H_5OH_{(g)} + 6CuO_{(s)}\ \Delta H = 333{\cdot}5\ \text{kJ/mol} \quad (3)$$

Some important assessments can be done by looking at the global reaction. Firstly, the ΔH is still high compared to other reactions such as the traditional methanol synthesis from CO_2 hydrogenation ($\Delta H = -49.5$ kJ/mol), which explains why the ethanol productivity is rather low at the reaction conditions applied in this work. Secondly, as shown in Fig. 5b, a stepwise process is proposed since Cu acts as both catalyst and reactant to produce ethanol and in-situ H_2, respectively. The active sites in the metallic copper surface are being saturated due to adsorption of oxygen from water, forming a shell of Cu_xO, which is responsible for deactivating the catalyst very quickly. The oxygen can be removed by successive steps of H_2 feeding between reaction steps.

In an electrochemical system, the deactivation by the oxidation of the Cu electrode is not so evident because the potentials normally applied for CO_2 reduction to ethanol (< -0.7 V) are considerably more negative than those for Cu^+ and Cu^{2+} reduction ($Cu^+ + e \leftrightarrow Cu_{(s)}$, $E = +0.52$ V; $Cu^{2+} + 2e \leftrightarrow Cu_{(s)}$, $E = +0.34$ V). To optimize the stability of the Cu in the thermocatalytic CO_2 hydrogenation with water steam, increasing the H_2/H_2O ratio could be an interesting strategy to enhance the reducibility of Cu_xO. However, H_2-TPR shows that Cu oxide powder reduces only at temperatures over 250 °C (Fig. S10) and thus H_2 will not be able to reduce Cu_xO in the temperature range for ethanol synthesis

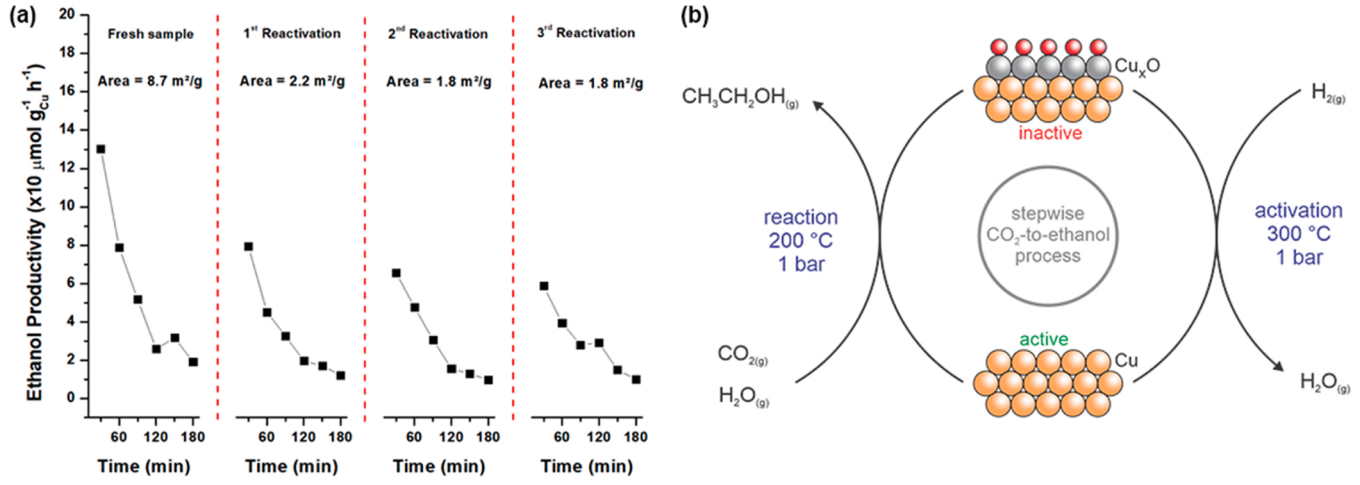

Fig. 5. (a) Ethanol productivity over time. Dashed red lines mean that a new reactivation of the Cu catalyst with H_2 at 300 °C was performed. (b) Proposed stepwise process model for CO_2-to-ethanol conversion over Cu catalyst.

(between 170 and 220 °C). Over 220 °C, better Cu reduction could be achieved but ethanol production would be suppressed, as shown in Fig. 2. Cu supported on oxides which lead for lower Cu temperature reduction must be considered for future studies. Therefore, water is a key component that acts both positively and negatively for ethanol synthesis from the hydrogenation of CO_2 with water steam. Finally, a natural question to be understood is why ethanol can be produced by adding water steam in the feed gas, but it is not formed when only CO_2 and H_2 are applied (Fig. S2). CO-DRIFTS experiments described in the next section give us an insight into the importance of the water steam in the reaction system.

3.4. CO-Drifts

Results have shown that ethanol can be synthesized from CO_2 hydrogenation in the presence of water steam, although the fundamental role of water in the process is unclear. CO-DRIFTS tests were carried out to understand how the adsorption of CO is influenced by the presence and absence of water steam. CO was chosen as a probe molecule since it is considered a key intermediate in the CO_2 hydrogenation and the reaction mechanism for C_{2+} synthesis. Previous tests (results not shown here) at standard conditions (15 °C) with monometallic Cu and catalysts with a high Cu loading (Cu/SiO_2, Cu/Al_2O_3, and Cu/CeO_2 with molar ratio of Cu/(SiO_2 or Al_2O_3) = 1/1) were carried out, and no signals referring to the CO bands were detected after the purging step with N_2. Therefore, monometallic Cu or catalysts with a high Cu loading could not be employed at the investigated conditions, requiring tests at very low temperatures [60]. However, at temperatures below 0 °C, water steam would condense, and these tests could not be performed.

On the other hand, previous works show that the application of a catalyst with low Cu loading supported on an oxide, such as the 2.5%Cu/CeO_2 compound, allows well-dispersed Cu^+ nanoparticles to be formed during the catalyst synthesis and the chemisorption of CO on Cu^+ (Cu^+-CO) remains stable even after purging with an inert gas (N_2, Ar or He) [60–62]. As discussed before, Cu^+ is pointed out as active site for the methanol synthesis from CO_2 hydrogenation and it is likely that Cu^+ is also partially formed during the Cu oxidation via water reduction in the CO_2 hydrogenation with water steam. Therefore, for the spectroscopic tests, Cu/CeO_2 (2.5 molar% of Cu in CeO_2) was chosen as a model catalyst in order to increase the sensibility of CO adsorption on the Cu active phase in the presence and absence of water steam.

Fig. 6 shows the CO-DRIFTS results. Before CO adsorption, the CuO/CeO_2 catalyst was reduced in situ to Cu/CeO_2 with a flow of 30 mL/min of H_2 at 300 °C for 1 h. The background was obtained at 15 °C after 15 min of purging with N_2 after the reduction process. The spectrum shown in Fig. 6 consists of the profile after the background subtraction and the bands are related to the CO adsorption. Linear CO was detected at 2119 cm^{-1} with shoulders at 2138 cm^{-1} and 2095 cm^{-1}, in accord with the literature [60,63]. The bands were deconvoluted with Voigt adjustment, and the result is shown in Fig. 6b. The total fit (dashed curve in red) was adequately adjusted to the experimental signal (curve in black), with the residual signal (curve in green) representing the difference between the experimental curve and the fit being null. This adjustment made it possible to identify three well-defined bands of adsorbed CO, centered at 2139, 2120, and 2105 cm^{-1}. The main band at 2120 cm^{-1} is attributed to Cu^+–CO species, as shown by many authors [60,61,64,65]. In addition, Cu^0–CO species can also appear at the same wavenumber as Cu^+–CO and these two species can be distinguished by their stability, being CO adsorbed on Cu^0 easily removed during the purging [60,61]. In the present study, since the 2120 cm^{-1} band was highly stable to N_2 purge, it is more likely to be related to Cu^+–CO. The shoulders at 2139 cm^{-1} and 2105 cm^{-1} are pointed out to be dicarbonyl species of Cu^+-$(CO)_2$, characterized by symmetrical and antisymmetrical vibration modes [61,66].

To investigate the adsorption of CO on Cu/CeO_2 in the presence of H_2 or H_2O steam, the same procedure performed previously was applied, but with CO adsorbing together with either H_2 or H_2O steam and the spectra after 15 min of purging with N_2 are shown in Fig. 7a. The spectrum obtained by exposing the catalyst only to the CO flow was also added to the figure as a reference. No significant difference is identified by comparing the profiles of the Cu^+-CO and Cu^+-$(CO)_2$ bands for the CO adsorption on Cu/CeO_2 with and without hydrogen in the medium (red line and black line, respectively). On the other hand, in the presence of water (blue line), it can be observed that the adsorption bands referring to Cu^+-CO and Cu^+-$(CO)_2$ shifted to smaller wavenumbers. Fig. 7b, c, and d show the bands evidenced in the experiments with CO, CO + H_2, and CO + H_2O, respectively, deconvoluted by Voigt adjustment. It becomes clear that the Cu^+-CO and Cu^+-$(CO)_2$ bands, located at 2120, 2139, and 2105 cm^{-1}, respectively, in the tests with CO and CO + H_2, moved to 2110, 2120, and 2098 cm^{-1}, respectively, in the test with CO + H_2O. This shift means that lower energies were needed to promote the vibrations of the C-O stretching of the adsorbate on the catalyst surface due to a weakening of the carbon-oxygen bond referring to the CO adsorbed on Cu. Simultaneously with the weakening of the carbon-oxygen bond, the carbon-metal bond is strengthened. In this way, water seems to stabilize CO on the Cu surface. These results may

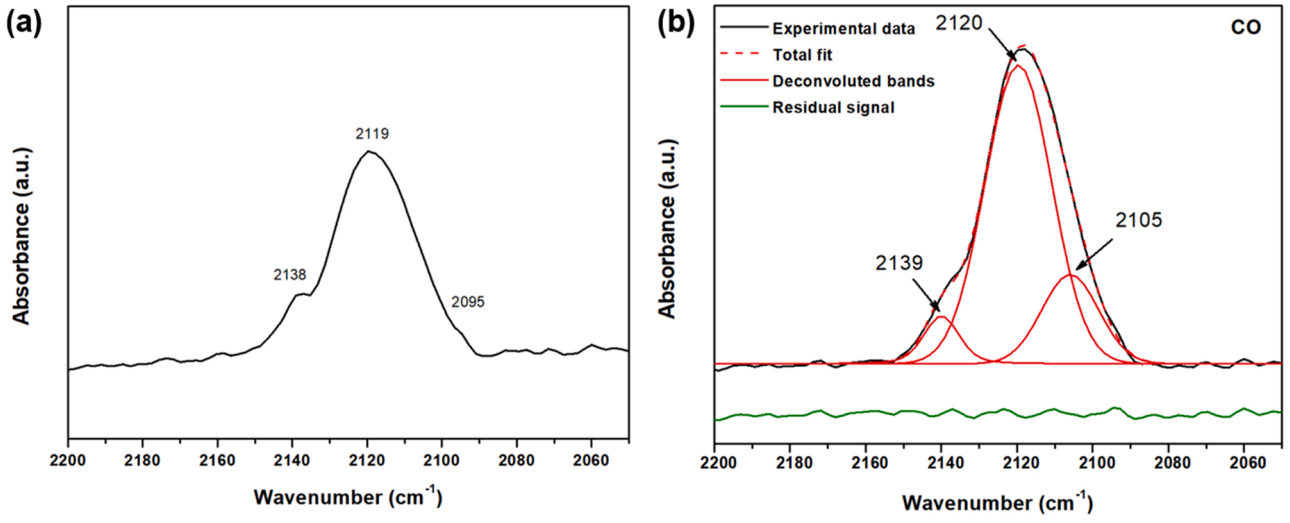

Fig. 6. (a) DRIFTS spectrum of CO adsorption on Cu/CeO_2 at 15 °C and atmospheric pressure followed by N_2 purge. (b) Deconvolution of the CO band by Voigt adjustment.

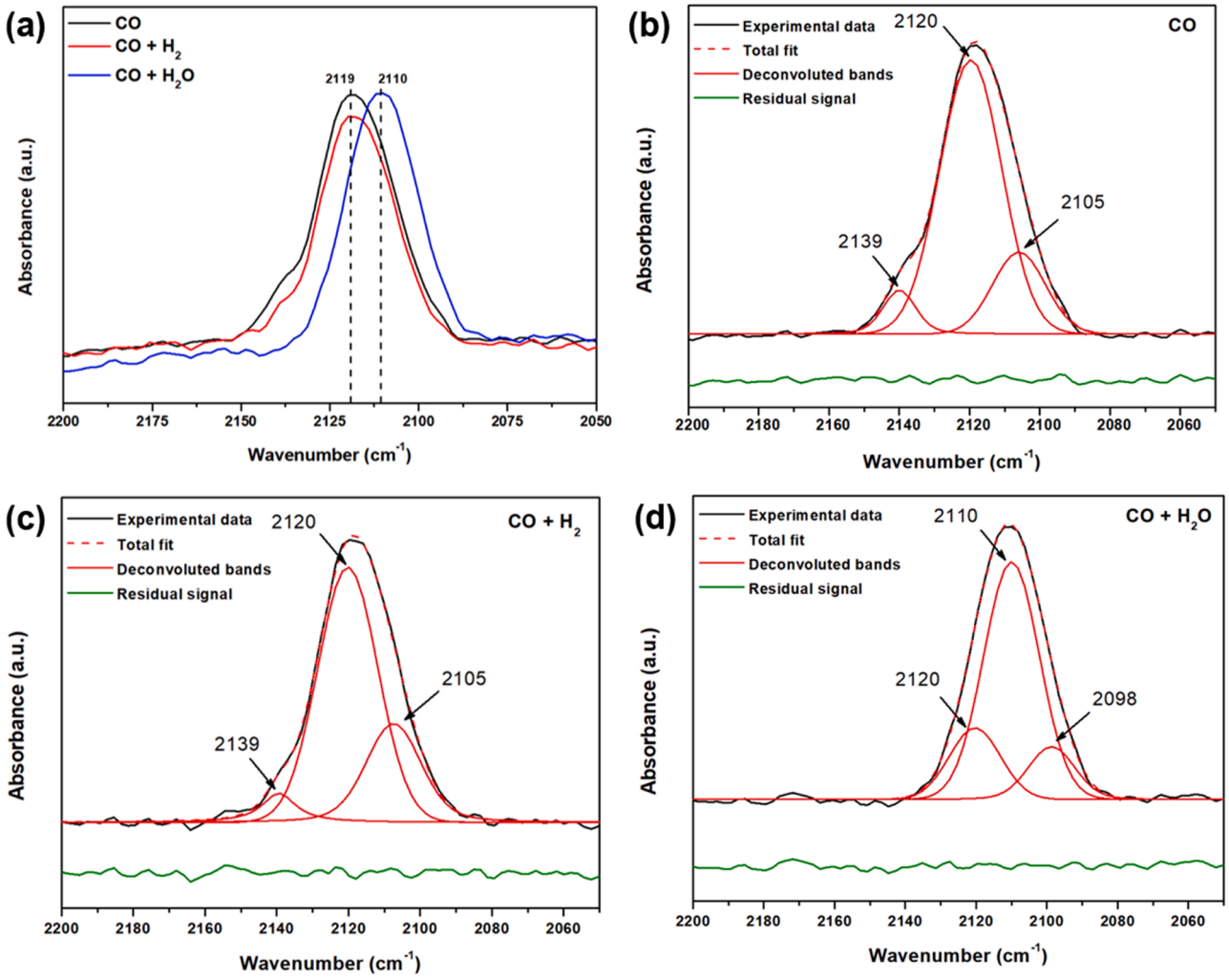

Fig. 7. (a) DRIFTS spectrum of CO (black curve), CO + H_2 (red curve), and CO + H_2O (blue curve) on Cu/CeO_2 at 15 °C and atmospheric pressure followed by N_2 purge. Deconvolution of the CO_{ad} band by Voigt adjustment when the tests were carried out with (b) CO; (c) CO + H_2; and (d) CO + H_2O.

explain why C_2 compounds are favored in the hydrogenation of CO_2 with water steam, whereas only C_1 compounds are observed when H_2 is used instead of water. As CO is considered a key intermediate in the synthesis of ethanol from CO_2, the strengthening of the carbon-metal bond, observed only in the CO adsorption tests with water steam, lead to maintaining CO adsorbed on the surface and, therefore, it is more

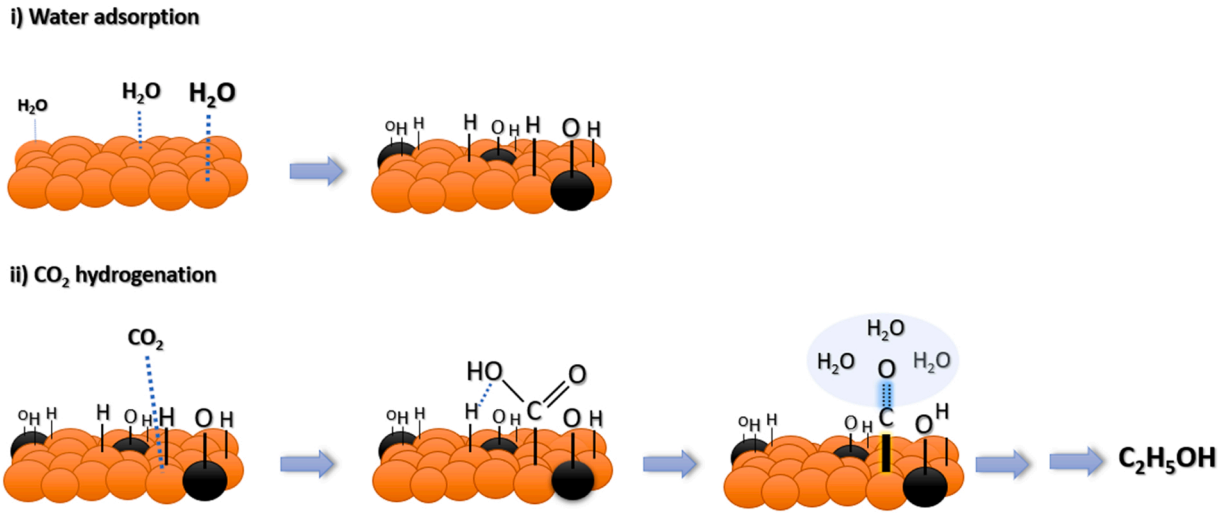

Fig. 8. Proposed scheme of (i) Water adsorption and (ii) CO_2 hydrogenation with water steam on Cu catalysts. The CO_2 adsorption is represented here on Cu and/or Cu^+.

likely that it continues to react rather than desorbing as a product.

A scheme representing the first steps of the reaction mechanism for ethanol synthesis from CO_2 and water steam is presented in Fig. 8, taking into account the catalytic results, thermodynamic discussion, and the DRIFTS tests. It is important to mention that CO_2 can adsorb in different ways depending on the catalyst and reaction conditions [67–69]. *HCOO is considered the main intermediate for methanol synthesis (called formate pathway) and it is believed that CO is not formed from this pathway [70]. *COOH is reported to be a common intermediate for CO formation as in the presence of H* , H_2O and CO are formed from the rupture of CO-OH [27,70]. The dissociative CO_2 adsorption (*CO+*O) is also reported to be a route for CO formation but *O must be consumed by *H to form *OH or H_2O and/or react with another *O to form O_2 [71]. Both dissociative CO_2 adsorption and *COOH may (simultaneously) happen, but as in our tests the system has a high concentration of water, and water can easily adsorb and oxidize the Cu surface (shown in Fig. 5), high concentration of H* will also be present on the Cu surface. For a representative scheme, the *COOH pathway was chosen here but further investigation must be done. In summary, one step consists of water adsorption and splitting on the Cu surface followed by its oxidation. Simultaneously, CO_2 is adsorbed on Cu and/or Cu^+ and further hydrogenated to CO. As shown by DRIFTS tests, a strengthening of the carbon-metal interaction is favored in the presence of water (represented by a thicker Cu-C bond). Finally, the most strongly adsorbed CO is further hydrogenated to ethanol.

4. Conclusions

Cu catalysts are not active for ethanol synthesis from CO_2 hydrogenation under standard conditions ($CO_2 + H_2$), although the opposite is observed in an electrochemical system ($CO_2 + H_2O$). Inspired by the electrochemical results, we showed that ethanol could be synthesized thermocatalytically by adding water steam in the feed gas ($CO_2 + H_2 + H_2O$) with selectivity of 84 % and productivity of ~2 $\mu mol.g_{cat}^{-1}.h^{-1}$. When only CO_2 and water steam were used, the same trend for ethanol synthesis was observed. This reaction showed to be both area- and crystalline structure- sensitive. Higher surface area and {100} facets showed better catalytic performance for ethanol synthesis. Applying deuterated water steam, it was possible to identify by ^1H NMR that water is acting as a hydrogen donor for the synthesis of ethanol. The direct synthesis of ethanol from CO_2 shows a high enthalpy value. Hence, the most likely reaction consists in the in-situ hydrogen formation by the oxidation of metallic copper while the water reduction occurs, followed by the hydrogenation of CO_2 into ethanol: 1) $6Cu_{(s)} + 6\,H_2O_{(g)} \rightarrow 6CuO_{(s)} + 6\,H_{2(g)}$; 2) $2CO_{2(g)} + 6\,H_{2(g)} \rightarrow C_2H_5OH_{(g)} + 3\,H_2O_{(g)}$. The low ethanol productivity evidenced in this work is explained by the high enthalpy ($\Delta H = 333.5$ kJ/mol) of the global reaction: $6Cu_{(s)} + 2CO_{2(g)} + 3\,H_2O_{(g)} \rightarrow C_2H_5OH_{(g)} + 6CuO_{(s)}$. By DRIFTS analysis, a strengthening of the carbon-metal interaction was observed only for the CO adsorption in presence of water steam, which may be one of the reasons why ethanol is favored in the CO_2 hydrogenation with water steam.

The approach used in this work for ethanol synthesis from CO_2 and water steam is far from a real application since the ethanol productivity and catalyst stability are rather low. However, this work opens new possibilities for future research related to CO_2 hydrogenation, considering the opportunity for high selectivity to higher alcohols by water enhancement. Using a feed gas mixture of CO_2, H_2, and H_2O over a catalyst more resistant to the water reduction (e.g., copper supported in oxides and multi-metallic materials) may be an interesting approach since better catalyst stability and the water-enhancement in carbon-metal strengthening can be both achieved simultaneously.

CRediT authorship contribution statement

Alisson H. M. da Silva: Conceptualization, Formal analysis, Investigation, Data curation, Writing – original draft, **Luiz H. Vieira**: Investigation, **Cássia S. Santana**: Investigation, **Marc T. M. Kopper**:– review & editing, Supervision, **Elisabete M. Assaf**:– Resources, review & editing, Supervision, **Janaina F. Gomes**: Conceptualization, Data Curation, Resources, Writing – review & editing, Supervision, **José M. Assaf**: Conceptualization, Recourses, Writing – review & editing, Supervision, Funding acquisition.

Declaration of Competing Interest

The authors declare that they have no known competing financial interests or personal relationships that could have appeared to influence the work reported in this paper.

Data availability

Data will be made available on request.

Acknowledgments

This work was supported by CNPq (grant number 141482/2016–8) and FAPESP (grant numbers: 2017/08420–0, 2015/06246–7, 2018/23601–3, 2017/05241–7, 2018/12021–6 and 2018/24339–0) and Research Center for Gas Innovation (RCGI-Shell-FAPESP grant 2020/15230–5).

Appendix A. Supporting information

Supplementary data associated with this article can be found in the online version at doi:10.1016/j.apcatb.2022.122221.

References

[1] M.Z. Ramli, S.S.A. Syed-Hassan, A. Hadi, Performance of Cu-Zn-Al-Zr catalyst prepared by ultrasonic spray precipitation technique in the synthesis of methanol via CO_2 hydrogenation, Fuel Process. Technol. 169 (2018) 191–198, https://doi.org/10.1016/j.fuproc.2017.10.004.

[2] X.-X. Hou, C.-H. Xu, Y.-L. Liu, J.-J. Li, X.-D. Hu, J. Liu, J.-Y. Liu, Q. Xu, Improved methanol synthesis from CO_2 hydrogenation over CuZnAlZr catalysts with precursor pre-activation by formaldehyde, J. Catal. 379 (2019) 147–153, https://doi.org/10.1016/j.jcat.2019.09.025.

[3] G. Wang, D. Mao, X. Guo, J. Yu, Methanol synthesis from CO_2 hydrogenation over CuO-ZnO-ZrO2-MxOy catalysts (M=Cr, Mo and W, Int. J. Hydrog. Energy 44 (2019) 4197–4207, https://doi.org/10.1016/j.ijhydene.2018.12.131.

[4] F.C.F. Marcos, L. Lin, L.E. Betancourt, S.D. Senanayake, J.A. Rodriguez, J.M. Assaf, R. Giudici, E.M. Assaf, Insights into the methanol synthesis mechanism via CO_2 hydrogenation over Cu-ZnO-ZrO2 catalysts: Effects of surfactant/Cu-Zn-Zr molar ratio, J. CO_2 Util. 41 (2020), https://doi.org/10.1016/j.jcou.2020.101215.

[5] H. Chen, H. Cui, Y. Lv, P. Liu, F. Hao, W. Xiong, H. Luo, CO_2 hydrogenation to methanol over Cu/ZnO/ZrO2 catalysts: Effects of ZnO morphology and oxygen vacancy, Fuel 314 (2022), https://doi.org/10.1016/j.fuel.2021.123035.

[6] H. Ban, C. Li, K. Asami, K. Fujimoto, Influence of rare-earth elements (La, Ce, Nd and Pr) on the performance of Cu/Zn/Zr catalyst for CH3OH synthesis from CO_2, Catal. Commun. 54 (2014) 50–54, https://doi.org/10.1016/j.catcom.2014.05.014.

[7] Z. Shi, Q. Tan, D. Wu, Enhanced CO_2 hydrogenation to methanol over TiO2 nanotubes-supported CuO-ZnO-CeO2 catalyst, Appl. Catal. A Gen. 581 (2019) 58–66, https://doi.org/10.1016/j.apcata.2019.05.019.

[8] J. Xiao, D. Mao, X. Guo, J. Yu, Effect of TiO2, ZrO2, and TiO2–ZrO2 on the performance of CuO–ZnO catalyst for CO_2 hydrogenation to methanol, Appl. Surf. Sci. 338 (2015) 146–153, https://doi.org/10.1016/j.apsusc.2015.02.122.

[9] D. Chen, D. Mao, J. Xiao, X. Guo, J. Yu, CO 2 hydrogenation to methanol over CuO–ZnO–TiO2–ZrO2: a comparison of catalysts prepared by sol–gel, solid-state reaction and solution-combustion, J. Sol-Gel Sci. Technol. 86 (2018) 719–730, https://doi.org/10.1007/s10971-018-4680-4.

[10] G. Noh, E. Lam, J.L. Alfke, K. Larmier, K. Searles, P. Wolf, C. Copéret, Selective hydrogenation of CO 2 to CH 3 OH on supported Cu nanoparticles promoted by isolated Ti IV surface sites on SiO 2, ChemSusChem 12 (2019) 968–972, https://doi.org/10.1002/cssc.201900134.

[11] M.M.-J. Li, Z. Zeng, F. Liao, X. Hong, S.C.E. Tsang, Enhanced CO_2 hydrogenation to methanol over CuZn nanoalloy in Ga modified Cu/ZnO catalysts, J. Catal. 343 (2016) 157–167, https://doi.org/10.1016/j.jcat.2016.03.020.

[12] W. Cai, P.R. de la Piscina, J. Toyir, N. Homs, CO_2 hydrogenation to methanol over CuZnGa catalysts prepared using microwave-assisted methods, Catal. Today 242 (2015) 193–199, https://doi.org/10.1016/j.cattod.2014.06.012.

[13] J. Cored, C.W. Lopes, L. Liu, J. Soriano, G. Agostini, B. Solsona, R. Sánchez-Tovar, P. Concepción, Cu-Ga3+-doped wurtzite ZnO interface as driving force for

enhanced methanol production in co-precipitated Cu/ZnO/Ga2O3 catalysts, J. Catal. 407 (2022), https://doi.org/10.1016/j.jcat.2022.01.032.
[14] C.S. Santana, L.S. Shine, L.H. Vieira, R.J. Passini, E.A. Urquieta-González, E. M. Assaf, J.F. Gomes, J.M. Assaf, Effect of the synthesis method on physicochemical properties and performance of Cu/ZnO/Nb_2O_5 catalysts for CO_2 hydrogenation to methanol, Ind. Eng. Chem. Res. 60 (2021), https://doi.org/10.1021/acs.iecr.1c02803.
[15] X. Jiang, X. Nie, X. Guo, C. Song, J.G. Chen, Recent advances in carbon dioxide hydrogenation to methanol via heterogeneous catalysis, Chem. Rev. 120 (2020) 7984–8034, https://doi.org/10.1021/acs.chemrev.9b00723.
[16] J. Niu, H. Liu, Y. Jin, B. Fan, W. Qi, J. Ran, Comprehensive review of Cu-based CO_2 hydrogenation to CH3OH: insights from experimental work and theoretical analysis, Int. J. Hydrog. Energy 47 (2022), https://doi.org/10.1016/j.ijhydene.2022.01.021.
[17] X. Jiang, N. Koizumi, X. Guo, C. Song, Bimetallic Pd–Cu catalysts for selective CO_2 hydrogenation to methanol, Appl. Catal. B 170–171 (2015) 173–185, https://doi.org/10.1016/j.apcatb.2015.01.010.
[18] F. Lin, X. Jiang, N. Boreriboon, Z. Wang, C. Song, K. Cen, Effects of supports on bimetallic Pd-Cu catalysts for CO_2 hydrogenation to methanol, Appl. Catal. A Gen. 585 (2019), 117210, https://doi.org/10.1016/j.apcata.2019.117210.
[19] A. Goeppert, M. Czaun, J.-P. Jones, G.K. Surya Prakash, G.A. Olah, Recycling of carbon dioxide to methanol and derived products – closing the loop, Chem. Soc. Rev. 43 (2014) 7995–8048, https://doi.org/10.1039/C4CS00122B.
[20] B.B. Asare Bediako, Q. Qian, B. Han, Synthesis of C_{2+} chemicals from CO_2 and H_2 via C–C bond formation, Acc. Chem. Res. 54 (2021) 2467–2476, https://doi.org/10.1021/acs.accounts.1c00091.
[21] Y. Lou, F. jiang, W. Zhu, L. Wang, T. Yao, S. Wang, B. Yang, B. Yang, Y. Zhu, X. Liu, CeO2 supported Pd dimers boosting CO_2 hydrogenation to ethanol, Appl. Catal. B. 291 (2021), 120122, https://doi.org/10.1016/j.apcatb.2021.120122.
[22] K. An, S. Zhang, H. Wang, N. Li, Z. Zhang, Y. Liu, Co0 − Coδ+ active pairs tailored by Ga-Al-O spinel for CO_2-to-ethanol synthesis, Chem. Eng. J. 433 (2022), 134606, https://doi.org/10.1016/j.cej.2022.134606.
[23] X. Ye, C. Yang, X. Pan, J. Ma, Y. Zhang, Y. Ren, X. Liu, L. Li, Y. Huang, Highly selective hydrogenation of CO_2 to ethanol via designed bifunctional Ir_1–In_2O_3 single-atom catalyst, J. Am. Chem. Soc. 142 (2020) 19001–19005, https://doi.org/10.1021/jacs.0c08607.
[24] L. Wang, S. He, L. Wang, Y. Lei, X. Meng, F.-S. Xiao, Cobalt–nickel catalysts for selective hydrogenation of carbon dioxide into ethanol, ACS Catal. 9 (2019) 11335–11340, https://doi.org/10.1021/acscatal.9b04187.
[25] L. Ding, T. Shi, J. Gu, Y. Cui, Z. Zhang, C. Yang, T. Chen, M. Lin, P. Wang, N. Xue, L. Peng, X. Guo, Y. Zhu, Z. Chen, W. Ding, CO_2 hydrogenation to ethanol over Cu@Na-Beta, Chem 6 (2020) 2673–2689, https://doi.org/10.1016/j.chempr.2020.07.001.
[26] Y. Wang, K. Wang, B. Zhang, X. Peng, X. Gao, G. Yang, H. Hu, M. Wu, N. Tsubaki, Direct conversion of CO_2 to ethanol boosted by intimacy-sensitive multifunctional catalysts, ACS Catal. 11 (2021) 11742–11753, https://doi.org/10.1021/acscatal.1c01504.
[27] S. Bai, Q. Shao, P. Wang, Q. Dai, X. Wang, X. Huang, Highly active and selective hydrogenation of CO_2 to ethanol by ordered Pd–Cu nanoparticles, J. Am. Chem. Soc. 139 (2017) 6827–6830, https://doi.org/10.1021/jacs.7b03101.
[28] D.L.S. Nieskens, D. Ferrari, Y. Liu, R. Kolonko, The conversion of carbon dioxide and hydrogen into methanol and higher alcohols, Catal. Commun. 14 (2011) 111–113, https://doi.org/10.1016/j.catcom.2011.07.020.
[29] S. Li, H. Guo, C. Luo, H. Zhang, L. Xiong, X. Chen, L. Ma, Effect of iron promoter on structure and performance of K/Cu–Zn catalyst for higher alcohols synthesis from CO_2 hydrogenation, Catal. Lett. 143 (2013) 345–355, https://doi.org/10.1007/s10562-013-0977-7.
[30] H. Kusama, K. Okabe, K. Sayama, H. Arakawa, Ethanol synthesis by catalytic hydrogenation of CO_2 over RhFeSiO2 catalysts, Energy 22 (1997) 343–348, https://doi.org/10.1016/S0360-5442(96)00095-3.
[31] G. Centi, S. Perathoner, A. Salladini, G. Iaquaniello, Economics of CO_2 utilization: a critical analysis, Front Energy Res. 8 (2020), https://doi.org/10.3389/fenrg.2020.567986.
[32] Y.Y. Birdja, E. Pérez-Gallent, M.C. Figueiredo, A.J. Göttle, F. Calle-Vallejo, M.T. M. Koper, Advances and challenges in understanding the electrocatalytic conversion of carbon dioxide to fuels, Nat. Energy 4 (2019) 732–745, https://doi.org/10.1038/s41560-019-0450-y.
[33] S. Nitopi, E. Bertheussen, S.B. Scott, X. Liu, A.K. Engstfeld, S. Horch, B. Seger, I.E. L. Stephens, K. Chan, C. Hahn, J.K. Nørskov, T.F. Jaramillo, I. Chorkendorff, Progress and perspectives of electrochemical CO 2 reduction on copper in aqueous electrolyte, Chem. Rev. 119 (2019) 7610–7672, https://doi.org/10.1021/acs.chemrev.8b00705.
[34] A. Prašnikar, A. Pavlišič, F. Ruiz-Zepeda, J. Kovač, B. Likozar, Mechanisms of copper-based catalyst deactivation during CO 2 reduction to methanol, Ind. Eng. Chem. Res 58 (2019) 13021–13029, https://doi.org/10.1021/acs.iecr.9b01898.
[35] B. Liang, J. Ma, X. Su, C. Yang, H. Duan, H. Zhou, S. Deng, L. Li, Y. Huang, Investigation on deactivation of Cu/ZnO/Al 2 O 3 catalyst for CO 2 hydrogenation to methanol, Ind. Eng. Chem. Res. 58 (2019) 9030–9037, https://doi.org/10.1021/acs.iecr.9b01546.
[36] Z. He, Q. Qian, J. Ma, Q. Meng, H. Zhou, J. Song, Z. Liu, B. Han, Water-enhanced synthesis of higher alcohols from CO 2 hydrogenation over a Pt/Co 3 O 4 catalyst under milder conditions, Angew. Chem. Int. Ed. 55 (2016) 737–741, https://doi.org/10.1002/anie.201507585.
[37] B. Zhao, Y. Liu, Z. Zhu, H. Guo, X. Ma, Highly selective conversion of CO_2 into ethanol on Cu/ZnO/Al2O3 catalyst with the assistance of plasma, J. CO_2 Util. 24 (2018) 34–39, https://doi.org/10.1016/j.jcou.2017.10.013.
[38] M. Behrens, F. Studt, I. Kasatkin, S. Kuhl, M. Havecker, F. Abild-Pedersen, S. Zander, F. Girgsdies, P. Kurr, B.-L. Kniep, M. Tovar, R.W. Fischer, J.K. Norskov, R. Schlogl, The active site of methanol synthesis over Cu/ZnO/Al2O3 industrial catalysts, Science 336 (2012) 893–897, https://doi.org/10.1126/science.1219831.
[39] E.L. Kunkes, F. Studt, F. Abild-Pedersen, R. Schlögl, M. Behrens, Hydrogenation of CO_2 to methanol and CO on Cu/ZnO/Al2O3: is there a common intermediate or not? J. Catal. 328 (2015) 43–48, https://doi.org/10.1016/j.jcat.2014.12.016.
[40] H. Ruland, H. Song, D. Laudenschleger, S. Stürmer, S. Schmidt, J. He, K. Kähler, M. Muhler, R. Schlögl, CO 2 hydrogenation with Cu/ZnO/Al 2 O 3: a benchmark study, ChemCatChem 12 (2020) 3216–3222, https://doi.org/10.1002/cctc.202000195.
[41] A. Koishybay, D.F. Shantz, Water is the oxygen source for methanol produced in partial oxidation of methane in a flow reactor over Cu-SSZ-13, J. Am. Chem. Soc. 142 (2020) 11962–11966, https://doi.org/10.1021/jacs.0c03283.
[42] Y. Wang, W. Gao, K. Li, Y. Zheng, Z. Xie, W. Na, J.G. Chen, H. Wang, Strong evidence of the role of H2O in affecting methanol selectivity from CO_2 hydrogenation over Cu-ZnO-ZrO2, Chem 6 (2020), https://doi.org/10.1016/j.chempr.2019.10.023.
[43] I.-C. Chang, P.-C. Chen, M.-C. Tsai, T.-T. Chen, M.-H. Yang, H.-T. Chiu, C.-Y. Lee, Large-scale synthesis of uniform Cu2O nanocubes with tunable sizes by in-situ nucleation, CrystEngComm 15 (2013) 2363, https://doi.org/10.1039/c3ce26932a.
[44] F.S. Roberts, K.P. Kuhl, A. Nilsson, High selectivity for ethylene from carbon dioxide reduction over copper nanocube electrocatalysts, Angew. Chem. 127 (2015) 5268–5271, https://doi.org/10.1002/ange.201412214.
[45] A.H.M. da Silva, S.J. Raaijman, C.S. Santana, J.M. Assaf, J.F. Gomes, M.T.M. Koper, Electrocatalytic CO_2 reduction to C2+ products on Cu and CuxZny electrodes: effects of chemical composition and surface morphology, J. Electroanal. Chem. 880 (2021), 114750, https://doi.org/10.1016/j.jelechem.2020.114750.
[46] C.W. Li, J. Ciston, M.W. Kanan, Electroreduction of carbon monoxide to liquid fuel on oxide-derived nanocrystalline copper, Nature 508 (2014) 504–507, https://doi.org/10.1038/nature13249.
[47] A. Verdaguer-Casadevall, C.W. Li, T.P. Johansson, S.B. Scott, J.T. McKeown, M. Kumar, I.E.L. Stephens, M.W. Kanan, I. Chorkendorff, Probing the active surface sites for CO reduction on oxide-derived copper electrocatalysts, J. Am. Chem. Soc. 137 (2015) 9808–9811, https://doi.org/10.1021/jacs.5b06227.
[48] R.-P. Ye, J. Ding, W. Gong, M.D. Argyle, Q. Zhong, Y. Wang, C.K. Russell, Z. Xu, A. G. Russell, Q. Li, M. Fan, Y.-G. Yao, CO_2 hydrogenation to high-value products via heterogeneous catalysis, Nat. Commun. 10 (2019) 5698, https://doi.org/10.1038/s41467-019-13638-9.
[49] F. Studt, M. Behrens, E.L. Kunkes, N. Thomas, S. Zander, A. Tarasov, J. Schumann, E. Frei, J.B. Varley, F. Abild-Pedersen, J.K. Nørskov, R. Schlögl, The mechanism of CO and CO 2 hydrogenation to methanol over Cu-based catalysts, ChemCatChem 7 (2015) 1105–1111, https://doi.org/10.1002/cctc.201500123.
[50] I.-C. Chang, P.-C. Chen, M.-C. Tsai, T.-T. Chen, M.-H. Yang, H.-T. Chiu, C.-Y. Lee, Large-scale synthesis of uniform Cu2O nanocubes with tunable sizes by in-situ nucleation, CrystEngComm 15 (2013) 2363, https://doi.org/10.1039/c3ce26932a.
[51] A.H.M. da Silva, S.J. Raaijaman, C.S. Santana, J.M. Assaf, J.F. Gomes, M.T. M. Koper, Electrocatalytic CO_2 reduction to C2+ products on Cu and CuxZny electrodes: effects of chemical composition and surface morphology, J. Electroanal. Chem. (2020), 114750, https://doi.org/10.1016/j.jelechem.2020.114750.
[52] F.S. Roberts, K.P. Kuhl, A. Nilsson, High selectivity for ethylene from carbon dioxide reduction over copper nanocube electrocatalysts, Angew. Chem. Int. Ed. 54 (2015) 5179–5182, https://doi.org/10.1002/anie.201412214.
[53] Y. Hori, I. Takahashi, O. Koga, N. Hoshi, Electrochemical reduction of carbon dioxide at various series of copper single crystal electrodes, J. Mol. Catal. A Chem. 199 (2003) 39–47, https://doi.org/10.1016/S1381-1169(03)00016-5.
[54] S. Saeidi, N.A.S. Amin, M.R. Rahimpour, Hydrogenation of CO_2 to value-added products – a review and potential future developments, J. CO_2 Util. 5 (2014) 66–81, https://doi.org/10.1016/j.jcou.2013.12.005.
[55] D. Xu, M. Ding, X. Hong, G. Liu, S.C.E. Tsang, Selective C 2+ alcohol synthesis from direct CO 2 hydrogenation over a Cs-promoted Cu-Fe-Zn catalyst, ACS Catal. 10 (2020) 5250–5260, https://doi.org/10.1021/acscatal.0c01184.
[56] A. Prašnikar, D.L. Jurković, B. Likozar, Reaction path analysis of CO_2 reduction to methanol through multisite microkinetic modelling over Cu/ZnO/Al2O3 catalysts, Appl. Catal. B 292 (2021), 120190, https://doi.org/10.1016/j.apcatb.2021.120190.
[57] A. Prašnikar, B. Likozar, Sulphur poisoning, water vapour and nitrogen dilution effects on copper-based catalyst dynamics, stability and deactivation during CO_2 reduction reactions to methanol, React. Chem. Eng. 7 (2022) 1073–1082, https://doi.org/10.1039/D1RE00486G.
[58] Z. Chen, H. Ge, P. Wang, J. Sun, M. Abbas, J. Chen, Insight into the deactivation mechanism of water on active Cu species for ester hydrogenation: experimental and theoretical study, Mol. Catal. 488 (2020), 110919, https://doi.org/10.1016/j.mcat.2020.110919.
[59] E. Shaaban, G. Li, Probing active sites for carbon oxides hydrogenation on Cu/TiO2 using infrared spectroscopy, Commun. Chem. 5 (2022) 32, https://doi.org/10.1038/s42004-022-00650-2.
[60] A. Hornés, P. Bera, A.L. Cámara, D. Gamarra, G. Munuera, A. Martínez-Arias, CO-TPR-DRIFTS-MS in situ study of CuO/Ce1−xTbxO2−y (x=0, 0.2 and 0.5) catalysts: support effects on redox properties and CO oxidation catalysis, J. Catal. 268 (2009) 367–375, https://doi.org/10.1016/j.jcat.2009.10.007.
[61] N.D. Subramanian, C.S.S.R. Kumar, K. Watanabe, P. Fischer, R. Tanaka, J.J. Spivey, A DRIFTS study of CO adsorption and hydrogenation on Cu-based core–shell nanoparticles, Catal. Sci. Technol. 2 (2012) 621, https://doi.org/10.1039/c2cy00413e.

[62] X. Wang, J.A. Rodriguez, J.C. Hanson, D. Gamarra, A. Martínez-Arias, M. Fernández-García, In situ studies of the active sites for the water gas shift reaction over Cu−CeO 2 catalysts: complex interaction between metallic copper and oxygen vacancies of ceria, J. Phys. Chem. B 110 (2006) 428–434, https://doi.org/10.1021/jp055467g.

[63] L. Yao, X. Shen, Y. Pan, Z. Peng, Synergy between active sites of Cu-In-Zr-O catalyst in CO_2 hydrogenation to methanol, J. Catal. 372 (2019), https://doi.org/10.1016/j.jcat.2019.02.021.

[64] K. Hadjiivanov, H. Knözinger, FTIR study of CO and NO adsorption and coadsorption on a Cu/SiO2 catalyst: probing the oxidation state of copper, Phys. Chem. Chem. Phys. 3 (2001) 1132–1137, https://doi.org/10.1039/b009649k.

[65] K. Hadjiivanov, T. Venkov, H. Knözinger, FTIR spectroscopic study of CO adsorption on Cu/SiO2: formation of new types of copper carbonyls, Catal. Lett. 75 (2001) 55–59, https://doi.org/10.1023/A:1016759123842.

[66] D. Scarano, S. Bordiga, C. Lamberti, G. Spoto, G. Ricchiardi, A. Zecchina, C. Otero Areán, FTIR study of the interaction of CO with pure and silica-supported copper(I) oxide, Surf. Sci. 411 (1998) 272–285, https://doi.org/10.1016/S0039-6028(98)00331-8.

[67] L.F. Rasteiro, R.A. de Sousa, L.H. Vieira, V.K. Ocampo-Restrepo, L.G. Verga, J. M. Assaf, J.L.F. da Silva, E.M. Assaf, Insights into the alloy-support synergistic effects for the CO_2 hydrogenation towards methanol on oxide-supported Ni5Ga3 catalysts: an experimental and DFT study, Appl. Catal. B. 302 (2022), 120842, https://doi.org/10.1016/j.apcatb.2021.120842.

[68] C.S. Santana, L.S. Shine, L.H. Vieira, R.J. Passini, E.A. Urquieta-González, E. M. Assaf, J.F. Gomes, J.M. Assaf, Effect of the synthesis method on physicochemical properties and performance of Cu/ZnO/Nb $_2$ O $_5$ catalysts for CO $_2$ hydrogenation to methanol, Ind. Eng. Chem. Res 60 (2021) 18750–18758, https://doi.org/10.1021/acs.iecr.1c02803.

[69] M.A. Rossi, L.H. Vieira, L.F. Rasteiro, M.A. Fraga, J.M. Assaf, E.M. Assaf, Promoting effects of indium doped Cu/CeO $_2$ catalysts on CO $_2$ hydrogenation to methanol, React. Chem. Eng. 7 (2022) 1589–1602, https://doi.org/10.1039/D2RE00033D.

[70] S. Kattel, B. Yan, Y. Yang, J.G. Chen, P. Liu, Optimizing binding energies of key intermediates for CO $_2$ hydrogenation to methanol over oxide-supported copper, J. Am. Chem. Soc. 138 (2016) 12440–12450, https://doi.org/10.1021/jacs.6b05791.

[71] J. Niu, H. Liu, Y. Jin, B. Fan, W. Qi, J. Ran, Comprehensive review of Cu-based CO_2 hydrogenation to CH3OH: insights from experimental work and theoretical analysis, Int J. Hydrog. Energy 47 (2022) 9183–9200, https://doi.org/10.1016/j.ijhydene.2022.01.021.